J. Plasma Fusion Res. SERIES, Vol. 11 (2015)

Hydrogen isotopes permeation in a fluoride molten salt for nuclear fusion blanket

Akira Nakamura, Satoshi Fukada and Ryosuke Nishiumi

Department of Advanced Energy Engineering Science, Kyushu University,
6-1 Kasuga-koen, Kasuga, Fukuoka 816-8580, JAPAN

(Received: 16 September 2014 / Accepted: 19 January 2015)

Mixed fluoride molten salts Flinak (LiF+NaF+KF) and Flibe (LiF+BeF_2) are expected to work as a tritium breeder in a fusion reactor blanket along with coolant and uranium fuel dissolver in a molten salt fission reactor. In this study, after making the molten salts in an electric furnace and purifying the salts by HF, experiments were performed to determine the behavior of H_2 permeation through the fluoride molten salts at static conditions in the range of 500-600 °C using an apparatus composed of tertiary cylindrical Monel400 tubes. In addition, transient H_2 diffusion equations in molten salts were solved, and results were compared with experimental effluent H_2 concentration curves. It is proved experimentally that the H_2 permeability through Flibe or Flinak has linear pressure dependence, and permeability, diffusivity and solubility of H_2 in the fluoride molten salts are correlated to their respective Arrhenius-type equations.

Keywords: molten salt, hydrogen isotopes, permeability, diffusivity, solubility

1. Introduction

For applications of a tritium breeding material to a nuclear fusion reactor, it is important to determine its hydrogen permeability, diffusivity and solubility in the breeding materials. In particular, fluoride molten salts are focused here due to comparatively easy handling, because their physical and chemical properties are appropriate. For example, they have high tritium breeding ratio, low reactivity with oxygen, low MHD pressure loss and their density and specific heat are almost the same as that of water. These properties are promising as a fusion blanket material. On the other hand, the melting point of a molten salt is higher than other liquid breeding materials. In recent years, a new fluoride molten salt mixture of LiF + NaF + BeF_2 called Flinabe is focused because the melting point was reported around 300 °C [1], which is around 100 °C lower than that of Flibe. However, there are few data relating to hydrogen behavior through Flibe, and Flinabe. Thus, the purpose of this report is to determine hydrogen behavior in the molten salts Flinak, and Flibe using a tertiary cylindrical tube system. Moreover, these data are also determined for preliminary experiment using Flinabe.

2. Experimental

Fig. 1 shows a schematic diagram of the experimental apparatus composed of a tertiary cylindrical tube system to determine the permeability, diffusivity and solubility of hydrogen in a molten salt. It is divided into two parts of the vessel storing a Ni crucible and a tertiary cylindrical tube system. First, the molten salt was purified by gas bubbling using gas including 1000 ppm hydrogen fluoride. The hydrogen fluoride concentration in the purge gas was measured by a pH meter after condensing in a sample flask. The melting point of the molten salts was measured by using an Inconel coating thermocouple inserted in the vessel. After purifying molten salts, it was moved into the tertiary cylindrical tube system that is made of 316 stainless-steel and Monel400 nickel alloy tube. The sectional view and the detail of the tertiary cylindrical tubes are shown in Fig. 2 and Table 1. The most internal pipe filled with hydrogen, and the molten salt is placed between 1st and 2nd tubes. The gas permeated to the outside pipe was purged by argon gas. The hydrogen concentration in the purge gas was detected by gas chromatography. These results were used for analyzing hydrogen permeability, diffusivity and solubility in each molten salt.

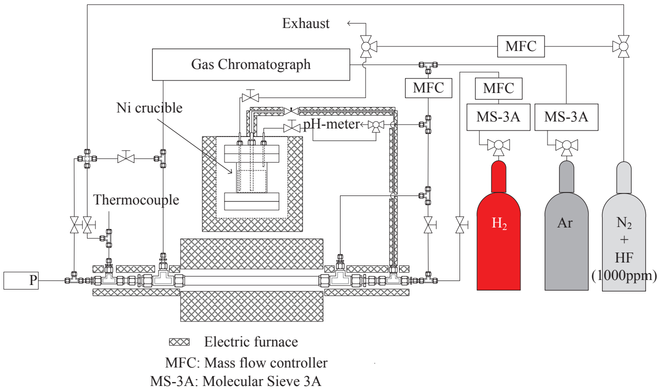

Fig. 1 A schematic diagram of the experimental apparatus composed of a vessel and tertiary cylindrical tubes.

---

a.nakamura@aees.kyushu-u.ac.jp

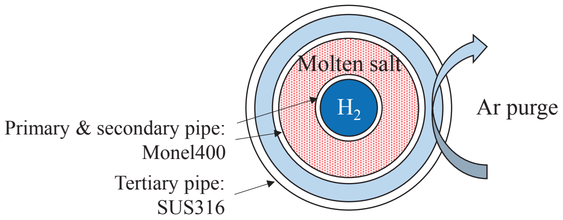

Fig. 2 A sectional view of the tertiary cylindrical tubes.

Table 1 The detail data of the tertiary cylindrical tubes.

	Component ratio (%)	Diameter (mm)	Thickness (mm)	Length (mm)
1st	65Ni-33Cu-2Fe	3.18	0.7	750
2nd	65Ni-33Cu-2Fe	12.7	1.0	530
3rd	18Cr-12Ni-2.5Mo	25.4	1.65	300

The outside diameter and thickness of 1st Monel-400 pipe are 3.18 mm and 0.7 mm. Those of 2nd pipe are 12.7 mm and 1.0 mm, and those of 3rd pipe are 25.4 mm and 1.65 mm. Thus, the thickness of the molten salt is 3.76 mm and the permeation area is 8.4×10^{-3} m^2. The argon flow rate was maintained at 30 cm^3/min. The temperature ranges 500-600 °C. Preliminary experiment was performed under conditions without the molten salt in order to determine the rate of hydrogen permeation through the Monel alloy. The temperature distribution of the tertiary cylindrical tubes and soundness of apparatus were confirmed. Table 2 shows the component ratio of the molten salt made for this experiment.

Table 2 Component ratio of each molten salt.

Molten salt	Component ratio (%)
Flinak	46.5LiF-11.5NaF-42KF
Flibe	67.2LiF-32.8BeF_2

3. Analysis

Transient hydrogen diffusion behavior was analyzed using the rectangular coordinate system for simplicity. A one-dimensional unsteady diffusion equation is described as follows:

$$\frac{\partial c}{\partial t}=D_{H_2}\frac{\partial^2 c}{\partial x^2} \tag{1}$$

where c [mol/m^3] is the molar concentration of hydrogen, D_H [m^2/s] is the diffusivity of hydrogen in the molten salt, x [m] is the direction perpendicular to surface of the molten salt layer and t [sec] is time. The initial and boundary conditions are as follows:

$$t=0,\ c=0, \tag{2a}$$

$$x=0,\ c=c_0, \tag{2b}$$

$$x=\ell,\ -D_{H_2}\frac{\partial c}{\partial x}=\frac{W}{K_{H_2}p_t A}c=Kc, \tag{2c}$$

where W [mol/s] is the molar flow rate of argon purge gas, K_H [mol/(m^3Pa)] is the Henry's constant, p_t [Pa] is the total pressure of purge gas, A [m^2] is the permeation area. Then the steady state permeation flux, j_H [mol/(m^2s)], is given by

$$j_{H_2}=\frac{D_{H_2}\cdot K_{H_2}}{L}\left(p_{H_2,up}-p_{H_2,down}\right) \tag{3}$$

where L [m] is the thickness of the molten salt, $p_{H_2,up}$ and $p_{H_2,down}$ [Pa] are the hydrogen partial pressures at upstream and downstream sides, respectively. The hydrogen permeability through molten salt, P_{H2}, becomes a product of the diffusivity and the solubility as follows:

$$P_{H_2}=D_{H_2}\cdot K_{H_2} \tag{4}$$

An analytical solution to Eq. (1) for H_2 permeation through a molten salt is expressed as follows:

$$j_{H_2}=\frac{c_0K}{1+\frac{KL}{D}}+\sum_{n=1}^{\infty}\frac{2c_0K}{\left(1+\frac{KL}{D}+\frac{D}{KL}\omega_n^2\right)\cos\omega_n}\times\exp\left(-\omega_n^2\frac{Dt}{L^2}\right) \tag{5}$$

These equations are used to determine the hydrogen permeability, diffusivity and solubility from experimental data.

4. Results and discussion

4.1 Purification and a melting point

Flibe needs to be purified because BeF_2 includes a small amount of BeO as impurities. To reduce BeO to BeF_2, the following chemical reaction is used:

$$BeO+2HF\rightarrow BeF_2+H_2O \tag{6}$$

Thus, Flibe is highly purified by HF bubbling. Fig. 3 shows the cooling curve of Flinak and Flibe. Two curves on Flibe are compared between cooling curves before and after the purification. From these results, the melting point of Flinak was measured 450±2 °C. that of Flibe is also measured 450±2 °C. These value are comparable to the reference data of $T_{\mathrm{LiF46.5\text{-}NaF11.5\text{-}KF42}}$ = 454 °C [3] and $T_{\mathrm{LiF67.2\text{-}BeF_232.8}}$ = 459 °C [4]. There are slight difference

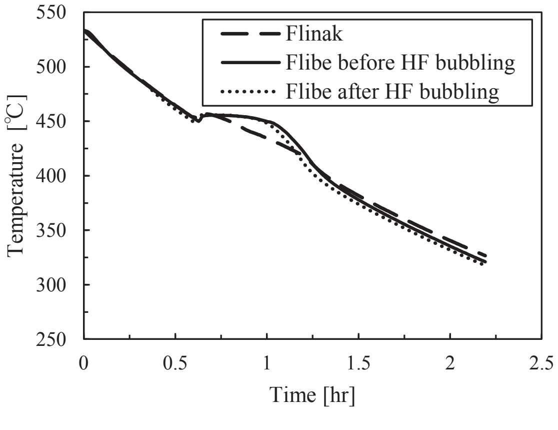

Fig. 3 Cooling curve of Flinak and Flibe.

between results before and after HF bubbling. Thus, it was confirmed that BeO was efficiently reduced to BeF_2 by HF bubbling.

4.2 Hydrogen permeation experiment to determine permeability, diffusivity and solubility.

Fig. 4 shows comparison of hydrogen permeability of Monel400 between the experimental data and the previous reference [2]. It is found that these results are almost the same as the data of the reference. We confirmed that temperature is uniform in the apparatus.

Fig. 5 compares the results of hydrogen permeation flux in the experimental apparatus. Square marks shown in the blank experiment, which corresponds to the Monel permeability, and the rest correspond to that of the molten salts, Flinak or Flibe, at 500 °C. This results shows that hydrogen permeation through the molten salt is the rate-determining process.

Fig. 6 shows the relationship between steady-state hydrogen permeation flux through Flibe, $(j_H)_{\text{steady-state}}$, and the upstream hydrogen partial pressure, $p_{H2,up}$ in the range from 10^4 to 6×10^5 Pa. In the experiment at 600 °C, it investigated only two pressure condition in 10^4 Pa and 3×10^5 Pa, because the experimental apparatus broke. Thus, the broken line virtually show the line of slope equals unity the same as 500 °C and 550 °C.

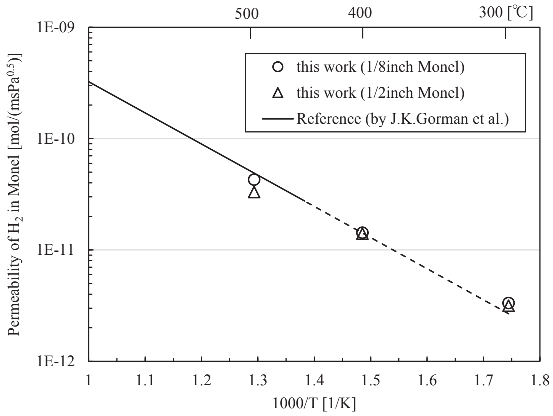

Fig. 4 Comparison of H_2 permeability of Monel between the present study and the previous ones.

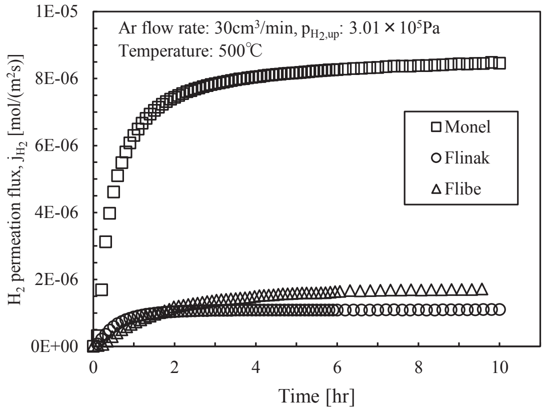

Fig. 5 Comparison between H_2 permeation flux of Monel and the molten salt, Flinak and Flibe.

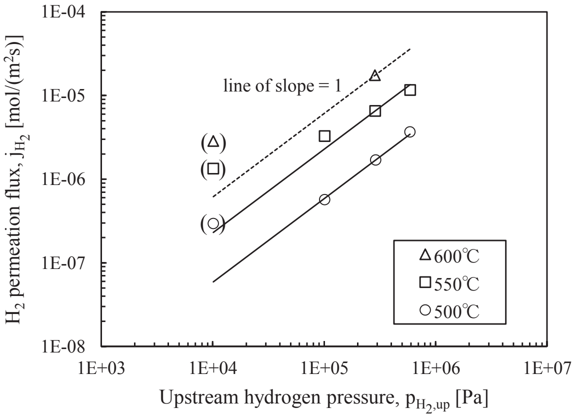

Fig. 6 The relationship between permeation flux and partial pressure of H_2 from 10^4 to 6×10^5 Pa.

The values of $(j_H)_{\text{steady-state}}$ are linearly proportional to the pressure, $p_{H2,up}$. The results proved experimentally the hydrogen sorption into Flibe obeys the Henry's law, which means hydrogen has moved through a molten salt in a molecular form. The reason why the result of j_H in 10^4 Pa is higher than others is that it used hydrogen (10%) and argon (90%) mixed gas, and the gas flows in slightly over atmospheric pressure condition, others are performed using pure hydrogen gas. The permeation flux is proportional to hydrogen partial pressure, this effect cannot explain the gap. However, it is considered that it is experimented under different conditions between 10^4 Pa and the range from 10^5 to 6×10^5 Pa due to the structure of this experimental apparatus. The effect of differential pressure between inlet and outlet gas may affect the gap. Therefore, it is concluded that permeation flux in Flibe is linearly proportional to the pressure using data of the range from 10^5 to 6×10^5 Pa.

Fig. 7 shows comparison of the hydrogen permeation flux in Flinak at 500 °C between experimental data and the analytical solution. The vertical axis represents the hydrogen permeation flux normalized by its steady state value. The horizontal axis represents normalized time.

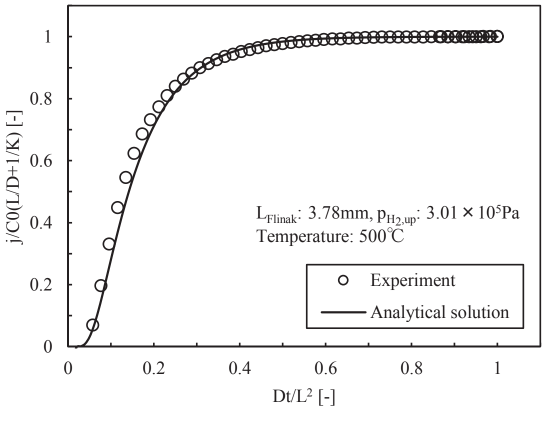

Fig. 7 Comparison of the H_2 permeation flux in Flinak between experiment and analytical solution.

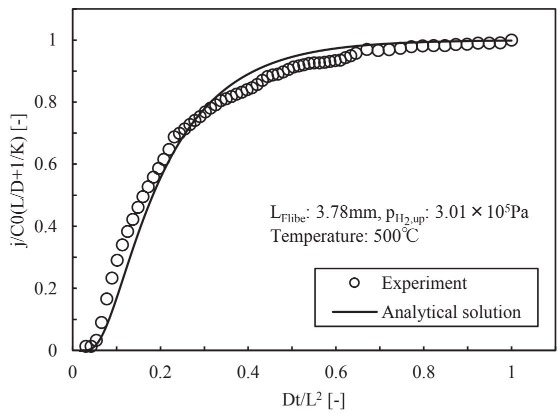

Fig. 8 Comparison of the H_2 permeation flux in Flibe between experiment and analytical solution.

Close agreement was obtained between experimental data and the analytical solution. The hydrogen diffusivity can be estimated from these results. The analysis at 550 °C and 600 °C is done in a similar way.

Fig. 8 shows comparison of the hydrogen permeation flux in Flibe at 500 °C between the experimental data and the analytical solution. Judging from this result, we confirmed that the analytical solution is almost in good against with the experimental data.

Fig. 9 shows a comparison of the permeability between Flinak and Flibe, and previous experimental data [5-7]. Our permeability data of Flinak and Flibe, P_{H2} [mol/msPa], are correlated to the following equations:

$$P_{Flinak-H_2} = 2.03\times10^{-9}\exp\left(-\frac{76.4[\mathrm{kJ/mol}]}{R_gT}\right) \tag{7}$$

$$P_{Flibe-H_2} = 1.37\times10^{-5}\exp\left(-\frac{129.7[\mathrm{kJ/mol}]}{R_gT}\right) \tag{8}$$

where R_g [J/mol] is the universal gas constant, and T is temperature in [K].

Fig. 10 shows a comparison of the diffusivity in Flinak and Flibe, and previous experimental data. The diffusivity data of hydrogen in Flinak and Flibe, D_{H2} [m^2/s], are correlated to the following equations:

$$D_{Flinak-H_2} = 3.59\times10^{-10}\exp\left(\frac{4.9[\mathrm{kJ/mol}]}{R_gT}\right) \tag{9}$$

$$D_{Flibe-H_2} = 2.09\times10^{-8}\exp\left(-\frac{25.2[\mathrm{kJ/mol}]}{R_gT}\right) \tag{10}$$

Fig. 11 shows a comparison of the solubility in Flinak and Flibe, and previous experimental data. The solubility data of hydrogen in Flinak and Flibe, K_{H2} [mol/m^{3}Pa], are calculated by Eq. (4) and correlated to the following equations:

$$K_{Flinak-H_2} = 5.64\exp\left(-\frac{81.3[\mathrm{kJ/mol}]}{R_gT}\right) \tag{11}$$

$$K_{Flibe-H_2} = 6.57\times10^{2}\exp\left(-\frac{104.8[\mathrm{kJ/mol}]}{R_gT}\right) \tag{12}$$

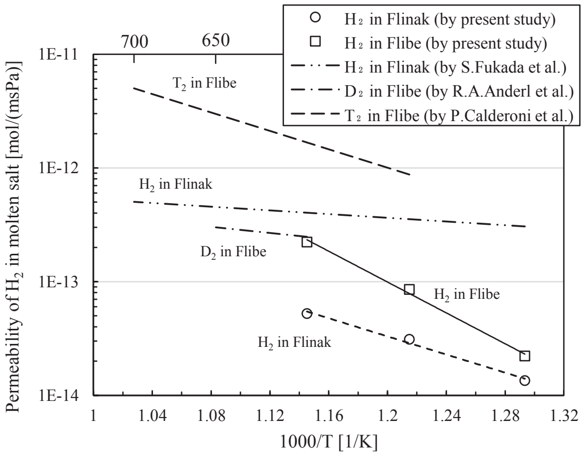

Fig. 9 Comparison of permeability of H_2 between the present study and previous ones.

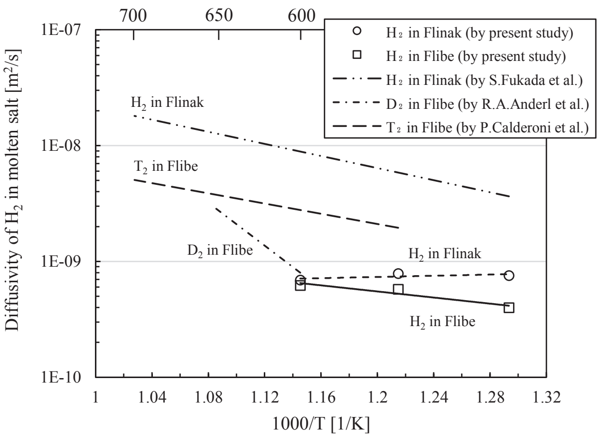

Fig. 10 Comparison of diffusivity of H_2 between the present study and previous ones.

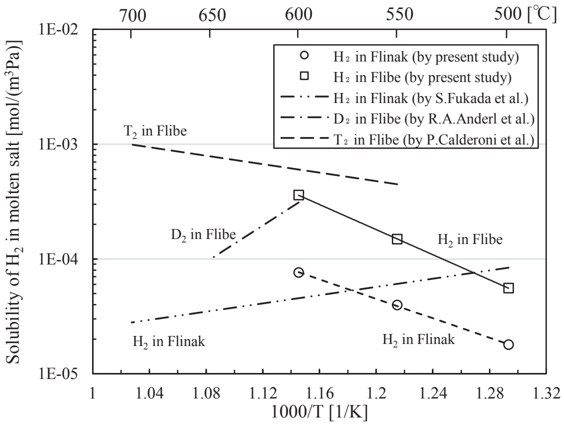

Fig. 11 Comparison of solubility of H_2 between the present study and previous ones.

There are one-order magnitude differences between previous reference data and the present ones, respectively. The difference may come from difference in permeation area or configuration of apparatus. Previous experiment is performed using almost the same. Another reason is the effect of impurities included in molten salt, and the other is the effect of temperature distribution. When the tertiary cylindrical tube is heated, three separate electric furnaces are used. According to these effects, the one-order magnitude difference may be observed. The activation energy for hydrogen permeation in Flinak is smaller than that of Flibe. It has been already proved by previous report [5] that it is affected by interaction with ions of respective components.

5. Conclusions

Hydrogen permeability, diffusivity and solubility in the molten salt Flinak and Flibe were determined by using a tertiary cylindrical tube system. The hydrogen solution in Flibe obeys the Henry's law. The analytical solution values are in good agreement with the experimental data. The hydrogen permeability in Flibe is higher than that in Flinak. The permeability, diffusivity and solubility obtained experimentally are correlated to the following equations, respectively:

$$Q_{i,H_2} = A_i \exp\left(-\frac{B_i\left[\text{kJ/mol}\right]}{R_g T} \right) \tag{13}$$

Table 3 The values of A_i and B_i appearing in Eq. (13)

Q	i = Flinak		i = Flibe	
	A_i	B_i	A_i	B_i
P	2.03×10^{-9}	76.4	1.37×10^{-5}	129.7
D	3.59×10^{-10}	-4.9	2.09×10^{-8}	25.2
K	5.64	81.3	6.57×10^{2}	104.8

6. References

[1] R. E. Nygren, *Fusion Sci. Technol.*, **47**, 549 (2005).
[2] J. K. Gorman et al., *vacuum*, **12**, 19 (19862).
[3] J. Lumsden, *Discuss. Faraday Soc.,* **32**, 138 (1961)
[4] K. A. Romberger et al., *J. Phys. Chem.*, **76**, 1154 (1972)
[5] S. Fukada et al., *J. Nucl. Mater.*, **358**, 235 (2006)
[6] R. A. Anderl et al., *J. Nucl. Mater.*, **329-333**, 1327 (2004)
[7] P. Calderoni et al., *Fusion Eng. Des.*, **83**, 1331 (2008)